33rd Annual International Conference of the IEEE EMBS
Boston, Massachusetts USA, August 30 - September 3, 2011

Nanostructured, highly aligned poly(hydroxy butyrate) electrospun fibers for differentiation of skeletal and cardiac muscle cells

Leonardo Ricotti, *Student Member , IEEE*, Alessandro Polini, Giada G. Genchi, Gianni Ciofani, *Member , IEEE*, Donata Iandolo, Virgilio Mattoli, *Member , IEEE*, Arianna Menciassi, *Member , IEEE*, Paolo Dario, *Fellow, IEEE,* Dario Pisignano

***Abstract*—The influence of novel nanostructured anisotropically electrospun poly(hydroxy butyrate) matrices on skeletal and cardiac muscle-like cell proliferation and differentiation was investigated, in comparison with isotropic and no-topographically cues-provided substrates. After the matrix characterization, in terms of surface SEM imaging and mechanical properties, cell differentiation on the different substrates was evaluated. Myogenin and F-actin staining at several differentiation time-points suggested that aligned nanofibers promote differentiation of both cell types. Moreover, quantitative parameters for each cell line are provided to clarify which aspects of the differentiation process are influenced by the different matrix topographies.**

I. Introduction

IT is well-known in the literature that cell behavior is strongly influenced by different topographies, and that some cues, more than others, can allow or enhance proliferation and differentiation processes [1], [2]. This is particularly true for muscle cells, whose orientation along one direction is of primary importance for the maximization of contractile force [3], and their capability to fuse into mature myotubes is differently affected by substrate micro- and nano-structuration, as reported in [4], [5]. Electrospinning is a versatile technique proved to be particularly useful for the production of scaffolds made by micro- or nano-fibers [6]. Interesting results have been obtained culturing skeletal muscle cells on electrospun parallel aligned nylon scaffolds [7], thus obtaining cell alignment and myotube development. However, the lack of scaffold degradability represents an obstacle for possible *in vivo* applications of such structures. Riboldi *et al*. described a novel degradable polyesterurethane (DegraPol®), electrospun in highly oriented microfibrous membranes, and they obtained good results in terms of skeletal muscle differentiation [8], [9]. The limit of such approach is the fiber size, that does not reach values smaller than 10 μm. As demonstrated by Wang *et al*. [5], in fact, the nanostructuration of the surface with submicron ridges and grooves allows a higher differentiation rate for these cells. Regarding cardiac muscle-like cells, polyaniline (PANi), a conductive, non-biodegradable polymer, has been blended with gelatin, co-electrospun into nanofibers and tested *in vitro* [10]. Only cell attachment and proliferation were investigated, finding a similar behavior on PANi electrospun matrices and on standard tissue culture-treated plastic. Focarete *et al*. cultured cardiac muscle cells on poly(ω-pentadecalactone) (PPDL) scaffolds, electrospun in nanofiber-based matrices, finding that such structures sustain cell attachment and proliferation [11].

As far as we know, no examples of differentiation of skeletal and cardiac muscle cells on biodegradable electrospun highly aligned nanofibers, having elastic modulus in the order of hundreds of MPa, can be found in the literature. In the present paper we describe the realization and characterization of highly aligned, nanofiber-based matrices of poly(hydroxy butyrate) (PHB), a biodegradable polyester produced by some bacteria [12]. We tested both skeletal and cardiac muscle-like cell lines on them, comparing the results with those obtained using electrospun isotropic matrices and flat PHB films. In particular, we evaluated myogenin expression after 1 day of differentiation and myotube development after 7 days of differentiation. From the analysis of fluorescent images, we extracted some quantitative parameters related to the differentiation level, thus highlighting some interesting differences for cells cultured on the different matrices.

Manuscript received June 20th, 2011.

L. Ricotti is with The BioRobotics Institute, Scuola Superiore Sant'Anna, and with the Center for Micro-Bio-Robotics @ SSSA, Istituto Italiano di Tecnologia, 56127, Pontedera (PI), Italy (corresponding author to provide phone: +39 050-883025; e-mail: l.ricotti@sssup.it).

A. Polini is with the NNL, National Nanotechnology Laboratory of Istituto Nanoscienze-CNR, and with the Scuola Superiore ISUFI, Università del Salento, 73100, Lecce, Italy (e-mail: alessandro.polini@nano.cnr.it).

G. G. Genchi is with the Biorobotics Institute, Scuola Superiore Sant'Anna, 56127, Pontedera (PI), Italy (e-mail: g.genchi@sssup.it).

G. Ciofani is with the Center for Micro-Bio-Robotics @ SSSA, Istituto Italiano di Tecnologia, 56127, Pontedera (PI), Italy (e-mail: g.ciofani@sssup.it).

D. Iandolo is with the NNL, National Nanotechnology Laboratory of Istituto Nanoscienze-CNR, 73100, Lecce, Italy (e-mail: donata.iandolo@nano.cnr.it).

V. Mattoli is with the Center for Micro-Bio-Robotics @ SSSA, Istituto Italiano di Tecnologia, 56127, Pontedera (PI), Italy (e-mail: virgilio.mattoli@iit.it).

A. Menciassi is with The BioRobotics Institute, Scuola Superiore Sant'Anna, and with the Center for Micro-Bio-Robotics @ SSSA, Istituto Italiano di Tecnologia, 56127, Pontedera (PI), Italy (e-mail: a.menciassi@sssup.it).

P. Dario is with The BioRobotics Institute, Scuola Superiore Sant'Anna, and with the Center for Micro-Bio-Robotics @ SSSA, Istituto Italiano di Tecnologia, 56127, Pontedera (PI), Italy (e-mail: p.dario@sssup.it).

D. Pisignano is with the NNL, National Nanotechnology Laboratory of Istituto Nanoscienze-CNR, and with the Dipartimento di Ingegneria dell'Innovazione, Università del Salento, 73100, Lecce, Italy (e-mail: dario.pisignano@unisalento.it).

II. Materials and Methods

A. Substrate preparation

Three different sample typologies were prepared: highly aligned PHB nanofibers (Aln-nF), random-oriented PHB nanofibers (R-nF), and flat PHB films (Flat). Aln-nF samples were prepared first dissolving PHB powder (Sigma) in hexafluoroisopropanol (HFIP, Carlo Erba), at a concentration of 33 mg/ml. The polymer solution was then loaded in a plastic syringe and a 4.5 kV voltage was applied using a high voltage power supply (EL60R0.6-22, Glassman High Voltage Inc.). An injection flow rate of 5 µl/min, and a deposition time of 60 min were used during electrospinning. A grounded rotating disk (RT Collector, Linari Engineering) was rotated at 17 m/s and used for Aln-nF deposition. The experiments were carried out at room temperature (relative humidity about 40%). R-nF samples were prepared using a static grounded collector, keeping constant the other operative parameters. Flat samples were obtained by spin coating, using the same polymer solution and glass coverslips as substrate. All the samples were maintained into a vacuum desiccator for one week at room temperature, to remove any residual of HFIP.

B. Matrix characterization

Scanning electron microscopy (SEM, Raith 150 system, Raith, Dortmund, Germany) investigation allowed for a first morphological characterization of sample surfaces. An acceleration voltage of 5 kV and an aperture size of 30 µm were used. A 10 nm metal layer was deposited on samples before SEM imaging, by Physical Vapour Deposition (PVD75, Kurt J. Lesker).

The mechanical properties of Aln-nF and R-nF samples were evaluated through traction tests measuring strain in response to unidirectional stress applied along the direction of higher parallelism of fibers. An INSTRON 4464 Mechanical Testing System was used with a ± 10 N load cell, and traction tests were performed on ten samples for each tested PHB typology. Samples were cut into 20 mm × 5 mm × 0.1 mm slices and allocated between two aluminum clamps. Traction force was applied along the fiber axis for the aligned nF samples, and along an arbitrary axis for random nF samples. All samples were pulled at the constant speed of 5 mm/min, until reaching sample failure. Data were acquired at a frequency of 100 Hz. The stress was calculated as the ratio between the load and the cross-section area of tensile specimens, while the strain was calculated as the ratio between the extension and the initial length of tensile specimens. The Young's modulus for each tested sample was calculated considering the stress/strain curve, and according to a standard procedure, as described in [13].

C. Cell cultures

C2C12 mouse myoblasts (CRL-1772, ATCC), and H9c2 embryonic rat myocardium cells (CRL-1446, ATCC) were used for cell experiments. Both cell lines were cultured using the same expansion medium, constituted by Dulbecco's modified Eagle's medium (DMEM) supplemented with 10% fetal bovine serum (FBS), 100 IU/ml penicillin, 100 µg/ml streptomycin and 2 mM L-glutamine. During culture, cells were maintained at 37°C in a saturated humidity atmosphere containing 95% air and 5% CO_2. Differentiation into myotubes was induced switching towards a differentiation medium, constituted by DMEM supplemented with 2 mM glutamine, 100 IU/ml penicillin, 100 µg/ml streptomycin, 1% Insulin-Transferrin-Sodium Selenite ([ITS] I3146; Sigma), and 1% FBS. Differentiation medium was replaced every day, and since the third day of differentiation, AraC 5 µg/ml (Pfizer) was added to the medium, in order to contrast persistent cell proliferation. Before cell seeding, all PHB specimens (5 × 5 mm) were sterilized with a streptomycin solution (2 mg/ml in PBS) for 30 min. Each specimen was then treated with a O_2 plasma (200 mTorr vacuum) for 60 s in a plasma cleaner and incubated with fibronectin (Sigma-Aldrich) at a concentration of 5 µg/cm^2 for 60 min at 37°C. Cells were seeded at a density suitable to reach confluence within 24 h.

D. Immunofluorescence (IF) staining

After 1 day of differentiation, the expression of myogenin, a characteristic protein of early muscle development [14], [15], was evaluated, according to the following procedure. Samples (3 for each matrix typology) were fixed with 4% paraformaldehyde (Sigma) in PBS for 15 min. After 3 rinses with PBS (5 min each), the cellular membranes were permeabilized with 0.1% Triton X-100 (Sigma) in PBS for 15 min. Aspecific binding sites were saturated with 10% goat serum (Gibco) in PBS for 15 min, and subsequently a primary antibody (rabbit polyclonal IgG, Santa Cruz) diluted 1:75 in 10% goat serum was added. After 30 min of incubation at 37°C, the samples were rinsed 5 times (3 min each) with 10% goat serum; then the staining solution, composed by a secondary antibody (fluorescent goat anti-rabbit IgG, Invitrogen) diluted 1:250 in 10% goat serum and by 1 µM DAPI, was added. After 30 min of incubation at room temperature, the samples were rinsed with 0.45 M NaCl in PBS for 1 min to remove weakly bound antibodies. After 3 rinses in PBS (5 min each), the samples were observed with an inverted fluorescent microscope and 5 pictures for each sample were taken at 10 × magnification.

After 7 days of differentiation, the arrangement of cytoskeleton f-actin was evaluated. The procedure was the same described before, but instead of adding primary and secondary antibodies, we added 1 µM DAPI (Invitrogen) and 100 µM Oregon Green® 488 phalloidin (Invitrogen) in PBS, for 30 min at room temperature. After that, samples were rinsed 3 times in PBS and observed by fluorescence microscopy. Five pictures for each sample were taken at 10 × magnification.

E. Extraction of differentiation indexes from fluorescence images

The collected images were elaborated with ImageJ, extracting the following parameters: (myogenin-positive)/(total nuclei) ratio, fusion index, myotube length, myotube width and myotube alignment. The (number of myogenin-positive nuclei)/(total number of nuclei) ratio was determined by counting, for each picture, the number of nuclei positive to myogenin staining (red-stained nuclei) and by dividing it by the total nuclei number (blue-stained).

The fusion index was determined by dividing, for each picture, the total number of nuclei in myotubes (≥ 2 nuclei) by the total number of counted nuclei. Myotube length and width were measured in each image. Myotube alignment was evaluated measuring the angle formed by each myotube with a preferential axis. The minimum myotube alignment value of 0° was chosen to correspond to unidirectionally oriented myotubes , while 90° to represent perpendicularly oriented myotubes. For Flat and R-nF samples, an arbitrary axis of alignment was chosen, while for Aln-nF samples the fiber axis was chosen as the alignment axis.

F. Statistics

The data underwent analysis of variance (ANOVA) to check differences among different samples, followed by *t*-test in case of comparison between two groups, and Holm-Sidak test in case of comparison among three or more groups. Significance was set at 5%.

III. Results

Fig. 1 shows the results of matrix characterization, in terms of surface morphology and mechanical properties.

A strong fiber alignment can be appreciated in Aln-nF samples, together with their submicron size. For both R-nF and Aln-nF samples the fiber diameter ranges from 240 up to 340 nm. Fiber alignment implies a higher elastic modulus and a greater ultimate tensile strength in comparison with random-oriented fibers samples, as revealed by stress-strain curves analysis of the tested specimens.

Myogenin staining images are shown in Fig. 2, and the quantification of (myogenin-positive nuclei)/(total nuclei) (PM/TN) ratio are reported in Table 1.

There is no difference among Flat and R-nF samples, in terms of myogenin expression, suggesting that the nanostructuration of the substrate does not significantly influence the differentiation. A higher PM/TN ratio is evident for Aln-nF samples, where fiber organization promotes a more efficient muscle differentiation at this stage. Later differentiation (7 days) was investigated by means of cytoskeleton actin staining. The most evident effect of aligned-fiber substrates on myotube development is related to their strong alignment along the fiber direction, but the different matrices also influence other parameters, as myotube length and width, *etc*.

To investigate this aspect, we extracted some quantitative parameters from the fluorescence images, providing a list of values that clarifies the influence of the different matrix topography on skeletal and cardiac muscle development (Table 2, *=p<0.05; **=p<0.001).

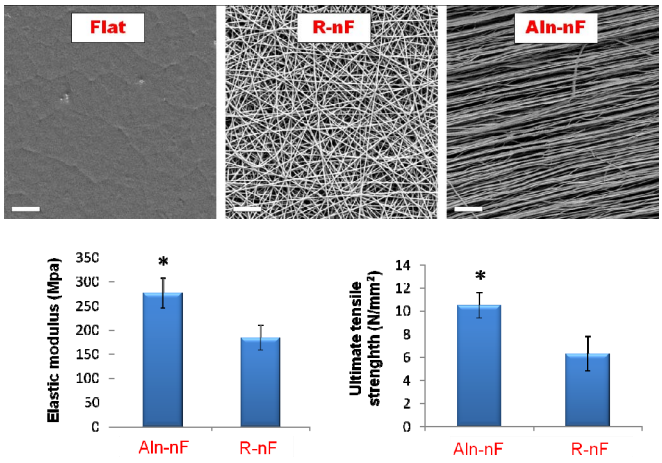

Fig. 1. Matrix characterization. SEM images of the three substrate typologies used in the study (top). Scale bar is 10 µm. Results of the traction tests on Aln-nF and R-nF samples (bottom). Elastic modulus and ultimate tensile strength values are reported. Tests were performed using 10 samples for each matrix typology.

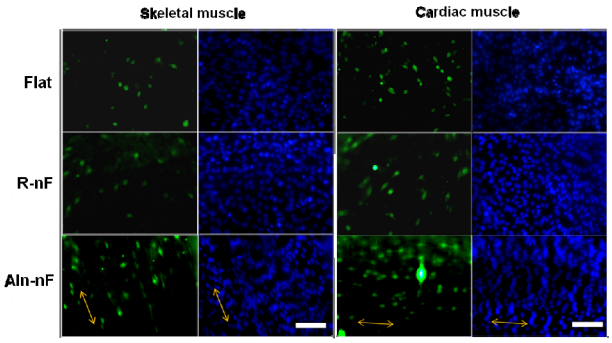

Fig. 2. IF images showing myogenin (in green) and nuclei (in blue) for the three sample typologies (Flat, R-nF, and Aln-nF) and for both cell types (skeletal and cardiac muscle). Scale bar is 100 µm. Yellow arrows show the alignment fiber direction for Aln-nF samples. The graph shows the (positive-myogenin)/(total nuclei) ratio values, calculated analyzing 5 images for each sample (experiment performed in triplicate).

The aligned fibers have a strong influence on the fusion index for both cell types. Concerning myotube length, Aln-nF samples induce longer myotube formation, and the effect is more pronounced for skeletal rather than for cardiac

TABLE I
PM/TN Ratio

	Skeletal muscle	Cardiac muscle
Flat	0.094 ± 0.008	0.014 ± 0.010
R-nF	0.099 ± 0.010	0.113 ± 0.006
Aln-nF	0.125 ± 0.006 (**)	0.132 ± 0.003 (*)

muscle cells. Myotube width is not appreciably affected by the substrate, even if, in all samples, the width values are smaller for skeletal muscle in comparison with cardiac muscle. Finally, Aln-nF topography strongly influences the alignment of both cell types.

IV. Conclusion

After a careful characterization of flat spin-coated PHB films, random-nanofiber-based and aligned-nanofiber-based matrices, we evaluated the differentiation of skeletal and cardiac muscle cells on such substrates. Myogenin expression was investigated by means of immunofluorescence, finding that on Aln-nF substrates such expression was significantly increased in comparison with cells cultured on the other matrices. Later differentiation (7 days) was investigated evaluating differentiation-related parameters after cytoskeleton actin imaging. We found that skeletal and cardiac muscle cells differently respond to the topographical stimuli used in this study, and we clarified which parameters of myotube development are more affected by matrix nanostructuration.

Envisioning further studies and possible applications of the described scaffolds, the culture of potentially implantable cell lines (such as induced Pluripotent Stem Cells) for tissue regeneration, and *in vivo* scaffold degradation profiles studies would be of great interest for the scientific community, as well as for clinical applications.

TABLE II
DIFFERENTIATION-RELATED PARAMETERS

Parameter	Measured value for skeletal muscle	Measured value for cardiac muscle
FUSION INDEX		
Flat	100 ± 8% [1]	100 ± 9% [4]
R-nF	114 ± 7% (*)	113 ± 6% (*)
Aln-nF	133 ± 8% (**)	164 ± 10% (**)
MYOTUBE LENGTH		
Flat	100 ± 11% [2]	100 ± 17% [5]
R-nF	105 ± 20%	108 ± 25%
Aln-nF	190 ± 12% (**)	179 ± 16% (*)
MYOTUBE WIDTH		
Flat	100 ± 13% [3]	100 ± 9% [6]
R-nF	107 ± 19%	104 ± 9%
Aln-nF	80 ± 25% (*)	91 ± 5%
DEVIATION FROM ALIGNMENT (°)		
Flat	41 ±13	47 ± 13
R-nF	45 ± 15	39 ± 9
Aln-nF	4 ± 2 (**)	3 ± 2 (**)

1 – 100% is 0.36
2 – 100% is 321 µm
3 – 100% is 15 µm
4 – 100% is 0.31
5 – 100% is 262 µm
6 – 100% is 22 µm

References

[1] J. Y. Wong, J. B. Leach, and X. Q. Brown, "Balance of chemistry, topography, and mechanics at the cell-biomaterial interface: issues and challenges for assessing the role of substrate mechanics on cell response," *Surf. Sci.*, vol. 570, issues 1-2, Oct. 2004, pp. 119-133.

[2] A. S. G. Curtis, and C. D. W. Wilkinson, "Reactions of cells to topography," *J Biomat. Sci. Polymer Edition*, vol. 9, number 12, 1998, pp. 1313-1329.

[3] T. Okano, S. Satoh, T. Oka, and T. Matsuda, "Tissue engineering of skeletal muscle: highly dense, highly oriented hybrid muscular tissues biomimicking native tissues," *ASAIO J,* vol. 43, 1997, pp. M749-M753.

[4] J. L. Charest, A. J. Garcia, and W. P. King, "Myoblast alignment and differentiation on cell culture substrates with microscale topography and model chemistries," *Biomaterials*, vol. 28, 2007, pp. 2202-2210.

[5] P. Y. Wang, H. T. Yu, and W. B. Tsai, "Modulation of alignment and differentiation of skeletal myoblasts by submicron ridges/grooves surface structure," *Biotechnol. Bioengineering*, vol. 106, 2010, pp. 285-294.

[6] K. Jayaraman, M. Kotaki, Y. Z. Zhang, X. M. Mo, and S. Ramakrishna, "Recent advances in polymer nanofibers," *J Nanosci. Nanotechnology*, vol. 4, 2004, pp. 52-65.

[7] A. Huber, A. Pickett, and K. M. Shakesheff, "Reconstruction of spatially oriented myotubes *in vitro* using electrospun, parallel microfiber arrays," *Eur. Cell. Materials*, vol. 14, 2007, 56-63.

[8] S. A. Riboldi, S. Sampaolesi, P. Neuenschwander, G. Cossu, and S. Mantero, "Electrospun degradable polyesterurethane membranes: potential scaffolds for skeletal muscle tissue engineering," *Biomaterials*, vol. 26, 2005, pp. 4606-4615.

[9] S. A. Riboldi, N. Sandr, L. Pigini, P. Neuenschwander, M. Simonet, P. Mognol, *et al*., "Skeletal myogenesis on highly orientated microfibrous polyesterurethane scaffolds," *J Biomed. Mat. Research*, vol. 84A, 2007, pp. 1094-1101.

[10] M. Li, Y. Guo, Y. Wei, A. G. MacDiarmid, and I. P. Lelkes, "Electrospinning polyaniline-contained gelatin nanofibers for tissue engineering application," Biomaterials, vol. 27, 2006, pp. 2705-2715.

[11] M. L. Focarete, C. Gualandi, M. Scandola, M. Govoni, E. Giordano, L. Foroni, *et al*., "Electrospun Scaffolds of a Polyhydroxyalkanoate Consisting of ω-Hydroxylpentadecanoate Repeat Units: Fabrication and In Vitro Biocompatibility Studies," *J Biomat. Science*, vol. 21, 2010, pp. 1283-1296.

[12] E. A. Dawes, and P. J. Senior, "The role and regulation of energy reserve polymers in micro-organisms," *Adv. Microbial. Physics*, vol. 10, 1973, 135-266.

[13] W. D. Callister, *Materials science and engineering, an introduction,* John Wiley & Sons, 2003. p 113-152.

[14] J. L. Moran, Y. Li, A. A. Hill, W. M. Mounts, and C. P. Miller, "Gene expression changes during mouse skeletal myoblast differentiation revealed by transcriptional profiling," *Phys. Genetics*, vol. 10, 2002, pp. 103-111.

[15] L. De Angelis, S. Borghi, R. Melchionna, L. Berghella, M. Baccarani-Contri, F. Parise, *et al*., "Inhibition of myogenesis by transforming growth factor β is density-dependent and related to the translocation of transcription factor MEF2 to the cytoplasm," *Proc. Natl. Acad. Science*, vol. 95, 1998, pp. 12358-12363.